Deep Recurrent Convolutional Neural Network for Fault Identification in Photovoltaic Panels using Thermal Imaging

K. Subha[1,*], S.Sharanya[1]

[1] SRM Institute of Science & Technology, Kattankulathur, India

Abstract **— Faults that are often invisible to existing inspection methods can significantly impact the reliability and efficiency of Photovoltaic (PV) systems. This study introduces an innovative framework for identifying PV panel faults using advanced machine learning algorithms and thermal images captured by unmanned aerial vehicles. The proposed Deep Recurrent Convolutional Neural Network (DRCNN) combines the strengths of Recurrent Neural Networks (RNNs) for learning temporal sequences and Convolutional Neural Networks (CNNs) for feature extraction. The DRCNN is designed to analyze thermal images of PV panels by capturing spatial and temporal patterns associated with fault-induced anomalies, such as hot spots, cracked cells or broken electrical connections. By leveraging CNN layers to extract critical features from thermal images and RNN layers to model the temporal dependencies and variations in thermal processes over time, the proposed approach integrates thermal image data collected under diverse environmental conditions. This dual strategy not only identifies faults based on spatial features but forecasts potential fault progression or the End-of-Life (EoL) for the panels by analyzing the evolution of thermal anomalies. The research aims to develop a highly accurate and efficient system for preventive maintenance and early problem detection, thereby improving the efficiency and durability of PV systems. The results demonstrate the DRCNN model's effectiveness in detecting various types of defects and delivering highly accurate real-time fault detection. By incorporating both spatial and temporal information, the proposed model significantly outperforms existing methods providing more robust and reliable defect identification.**

Index Terms **— Deep Recurrent Convolutional Neural Network, fault identification, hot spot detection, end-of-life prediction, proactive maintenance, predictive maintenance.**

I. Introduction

In modern society, electricity systems must operate reliably and efficiently. Key components of electricity systems, including generators, fuses, transmission lines, and PV panels, play a critical role in ensuring the smooth operation of these systems. Malfunctions in these components can lead to significant equipment damage and power outages, causing inconvenience and disruption [1]. Early detection of component failures is essential to mitigate the impact of outages on the electrical system [2]. Rapid identification and resolution of component issues are vital for the reliable and continuous operation of power systems. Early fault detection minimizes downtime, enhances system reliability, and improves customer satisfaction by enabling timely repairs and scheduled maintenance. Existing methods for identifying faults in power system components primarily rely on manual diagnostic techniques and periodic visual inspections [3]. These approaches have limitations in terms of flexibility, accuracy, and efficiency. Visual inspections may overlook hidden or early-stage defects and are prone to human error and subjective judgment. Manual diagnostics are time-intensive, require specialized expertise, and may not be suitable for large-scale systems [4].

* Corresponding author.
E-mail: k.subhabalamurugan@gmail.com

DOI:10.25729/esr.2025.03.0008

Received June 27, 2025. Revised October 27, 2025. Accepted September 1, 2025. Available online November 28, 2025.

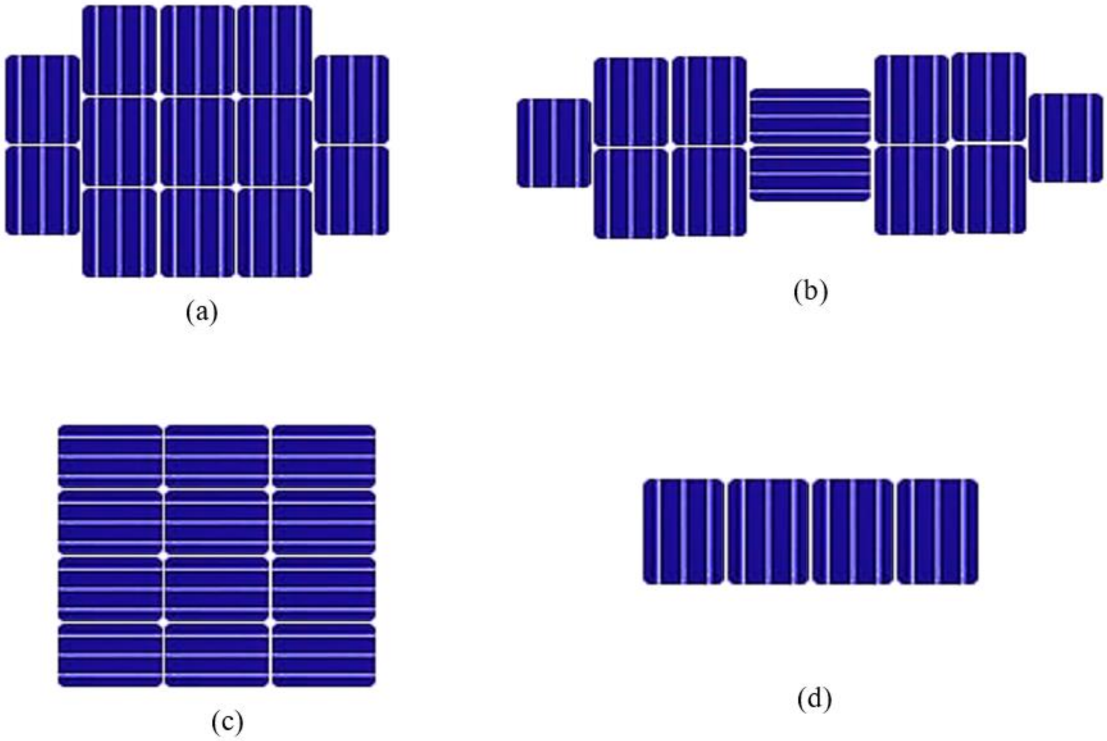

Fig. 1.Some PV solar tracker and panel setups.

To overcome these limitations, researchers and developers have turned to advanced techniques for improving the detection of faults in electrical system components. Infrared Thermography (IRT) is one such sophisticated method, which analyzes thermal characteristics by capturing thermal images of electrical system components. Abnormal temperature patterns or ranges can indicate potential component failures [5]. In addition to IRT, advanced data analysis methods, such as feature extraction and classification techniques, are employed to enhance fault detection accuracy and efficiency. These methods aim to classify collected thermal images into distinct fault categories and extract valuable insights from them. By leveraging data analysis and Artificial Intelligence (AI), the techniques automate the detection process, reducing human error, and managing large volumes of data in real time [6]. The growing demand for Renewable Energy Sources (RES), driven by ecological and climate concerns, along with the global economic recovery, poses significant challenges for the future. Reducing emissions and dependence on fossil fuels requires the adoption of alternative energy sources. Distributed PV plants are increasingly being deployed, and most of these systems are decentralized [7]. Europe has seen one of the most significant increases in this sector over the past five years, particularly in energy production from PV systems and RES. The importance of monitoring and maintaining PV plants grows, presenting challenges related to reliability, efficiency, durability, and safety. Several PV solar tracker and panel setups are depicted in Fig. 1 [8].

The durability and overall reliability of PV plants can significantly affect anticipated profits. The primary aim of this work is to address the fault identification challenge using the thermal images gathered through IRT. To achieve this, multiclass classification is employed for fault diagnosis, while binary classification is used for fault detection [9]. The literature indicates that various techniques were developed for this purpose. AI and advanced learning techniques are used to categorize typical red, green, blue (RGB) images of PV. Comparison of the *k*-nearest neighbors (kNN) classification algorithm with other classification methods demonstrates improved accuracy of up to 98.95% with a computation time of 0.04 seconds [10]. CNN-ML models are applied to identify PV issues by processing true-color images captured by Unmanned Aerial Vehicles (UAVs). The frameworks VGG16, GoogLeNet, AlexNet, and ResNet50 are evaluated in terms of their ability to extract relevant features. The study reveals that Support Vector Machine (SVM) classifiers exhibit the best performance for real-time classification in multi-class applications [11].

Information collected from two operational PV power plants in India facilitated the identification of specific connections between internal and external plant characteristic variables. Proposed IRT-based fault classification was used instead of signal processing for diagnosing PV failures [12]. The latest research in this area presents an automated defect identification system that leverages supervised machine learning techniques and texture feature extraction. To identify observable PV defects, a CNN-based deep learning framework with seven learned layers is employed. The study evaluates six common faults using an 8400-image dataset [13].

A. Problem Statement

Microcracks, electrical failures, and hotspots are among the issues that can significantly impair the efficiency of PV panels and reduce their lifespan. Existing analysis techniques such as electrical testing or manual visual inspections, are costly, time-consuming, and often ineffective at detecting minor or concealed flaws. Thermal imaging offers a non-invasive, efficient, and reliable method for identifying thermal anomalies caused by PV panel defects. Despite its potential, analyzing thermal images for fault diagnosis remains challenging due to complex, fluctuating climatic conditions and the precise, dynamic nature required for real-time fault detection in PV systems. Existing methods struggle to effectively evaluate temporal and spatial information, which is crucial for predicting the potential End-of-Life (EOL) for PV panels and detecting problems at an early stage. To facilitate preventive maintenance and enhance the reliability and longevity of solar energy systems, there is a need for an advanced, automated system capable of accurately detecting, categorizing, and predicting PV panel issues by using thermal imaging data.

B. Motivation

The increasing use of PV systems as an environmentally friendly energy source has highlighted the necessity of efficient and reliable maintenance processes to ensure their longevity and peak performance. Early failure detection is crucial for minimizing system downtime, reducing maintenance costs, and optimizing energy output as PV systems continue to proliferate. Existing defect detection techniques often require significant effort and are prone to human error, while struggling to keep pace with the growing complexity and scale of PV installations. Thermal

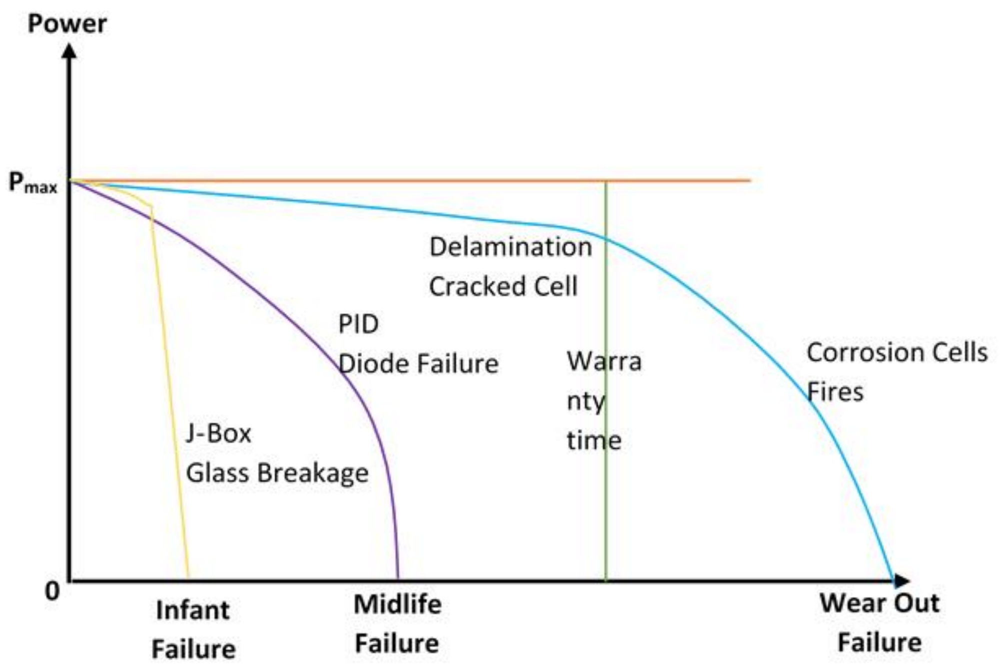

Fig. 2. Main categories of PV failures.

imaging provides a potential solution by enabling non-invasive, real-time identification of abnormalities that may indicate defects. The challenge lies in efficiently analyzing the vast amount of temperature data generated under varying external conditions. By addressing the limitations of existing techniques, this approach aims to provide a reliable, automated, proactive problem detection solution, thereby enhancing the efficiency, dependability, and management of PV systems.

II. RELATED WORKS

A research study on automated PV defect identification using realistically recorded IRT images in both indoor and outdoor settings is proposed in [14]. The study relies on deep learning approaches for independent ensemble transfer. The precision of a light CNN architecture-based, independently trained model achieved 98.67%. With independent and transferred learning systems, it took 13.12 ms and 13.07 ms, respectively, to generate an estimate for a single image. The computing cost required to achieve the model's effectiveness is not disclosed in the paper [15]. An IRT image-based method was developed that combined transfer learning with an Isolated Convolutional Neural Model (ICNM). Effectiveness indicators of the proposed multi-class classification method included validation loss, testing accuracy, training loss, training accuracy, and time to completion [16]. The PV health-based categorization findings were presented using the ICNM and publicly available pre-trained transfer learning models (SqueezeNet, GoogleNet, and ShuffleNet). Within the analysis, 695 images showed defects related to overheated regions, such as hotspots and overheating segments [17]. SC-DeepCNN was used to identify IRT images with hotspots. To recognize objects in hot areas an ROI-DeepCNN algorithm was created and applied in conjunction with joint learning. Thermal imaging provides a visual representation of the frequency patterns observed in the components. Various temperature indicators can be observed across different components, highlighting conditions such as normal operation, deterioration, soiling, fractures, short circuits, and other faults [18].

By analyzing the thermal properties of components, potential issues or abnormalities in PV systems can be detected at an early stage. Thermal imaging is a powerful tool that enables investigators to monitor the thermal behavior of components, revealing underlying problems or deviations from normal operations. A critical consideration in this process is the Field of View (FoV), which determines the spatial coverage of the thermal image, or the area captured by the thermal camera [19]. Choosing an appropriate FoV is therefore essential to ensure accurate data collection and processing. For instance, operational problems in PV modules can be categorized into three main groups based on the energy losses incurred: neonatal failures, midlife failures, and wear-out failures [20]. Neonatal failures occur during the initial operation of a PV system, often due to errors from manufacturers or installers, resulting in a rapid and significant decline in power output. In contrast, wear-out failures occur at the end of the PV module lifespan, typically when output drops to 80–70% of the initial energy, raising security and performance concerns [21]. The severity of PV defects further influences their categorization. Acute problems, such as short-circuit and open-circuit faults, are considered critical because they can cause complete shutdown of the energy system. On the other hand, chronic problems, often caused by partial shading or irregular light reception, are less severe but still impact overall efficiency [22]. Therefore, evaluating PV performance requires examining parameters such as light absorption, cell condition, and interconnections to promptly identify permanently defective components. Proper FoV selection is particularly important here, for thermal cameras to capture critical regions that are most likely to develop defects. This improves the reliability of datasets and strengthens fault diagnosis by covering both acute and chronic error regions [23].

Compared to existing methods, the proposed FoV-based thermal image collection framework emphasizes tailored data acquisition for PV systems. Existing approaches may overlook critical component regions or fail to adequately represent thermal behavior, thereby producing incomplete or less reliable data. By contrast, the FoV-based approach ensures a comprehensive and accurate representation of thermal properties, improving the precision of defect detection and analysis [24]. Researchers show that such targeted imaging significantly enhances fault identification, providing more representative datasets for training advanced models. Despite these improvements, several key limitations remain in current PV defect identification frameworks. Existing approaches often rely on shallow training algorithms or basic image-processing techniques, which lack the capability to capture the dynamic and complex nature of temperature anomalies in PV systems [25]. These methods are insufficient to detect subtle or evolving faults as they primarily exploit spatial

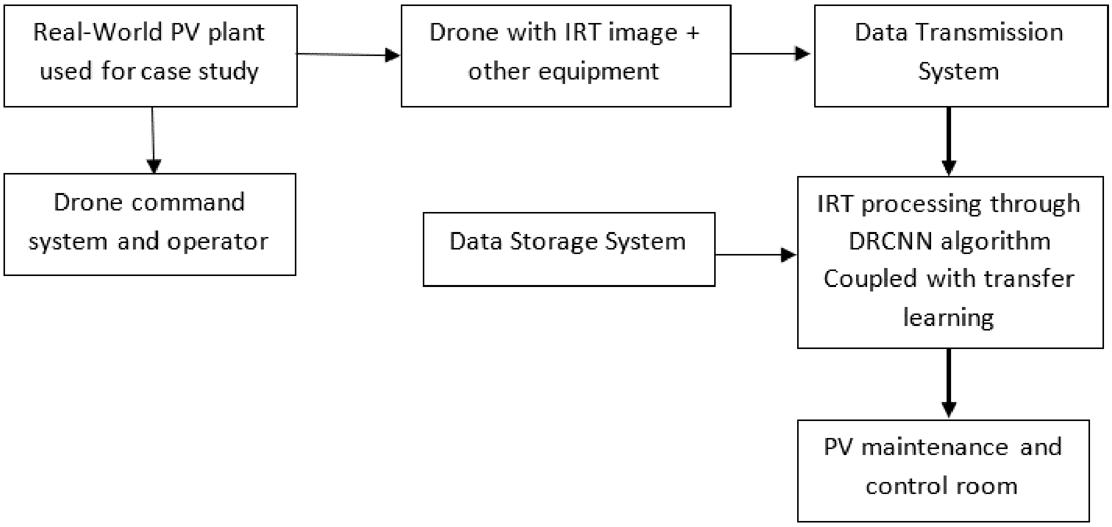

Fig. 3. Proposed architecture.

features while neglecting temporal dependencies critical for forecasting End-of-Life (EoL) states and tracking fault progression [26]. Thermal imaging data are highly sensitive to environmental factors such as fluctuating illumination and ambient temperature changes, yet existing systems are often not robust enough to address these variations [27]. This shortfall frequently results in delayed fault detection, reduced preventive maintenance capacity, and increased operational costs. To overcome these limitations, there is a need for a more integrated approach capable of handling both spatial and temporal dependencies, while accounting for environmental variations. Advanced deep learning architectures are well-suited to address these requirements. This study introduces a CNN designed to analyze thermal images comprehensively, track fault progression over time, and deliver early, accurate fault detection. By bridging spatial-temporal analysis with robust environmental adaptation, the proposed method addresses the gaps left by existing works and contributes to improving the long-term sustainability, reliability, and energy efficiency of PV systems [28,29].

III. Materials and Methods

The proposed method employs CNNs to identify abnormalities such as hot spots, microcracks, or overheated regions that may indicate issues by extracting spatial information from thermal images of PV panels shown in Fig. 3. Temporal analysis is crucial for understanding how defects develop, predicting their future impact, and determining the EoL of PV panels. The DRCNN technique is particularly beneficial for PV fault identification as it effectively handles the complexity of dynamic thermal images captured under varying environmental conditions, such as fluctuations in sunlight, temperature, or weather. By incorporating both spatial and temporal information, the DRCNN can detect faults at an early stage, including those that develop gradually or are difficult to identify in a single thermal image. This proposed system enhances the accuracy and efficiency of fault detection and enables proactive maintenance scheduling, reducing downtime, preventing severe malfunctions, and optimizing the overall efficiency of solar power systems. By integrating CNN and RNN methodologies, the proposed solution provides a robust, automated system for real-time fault detection in PV systems, thereby improving their operational lifespan and reliability.

A. Dataset Description

More than 10 000 thermal images taken by UAVs fitted with infrared thermographic cameras make up the dataset utilized for thermal imaging defect diagnosis in PV panels shown in Table 1. These images were taken from a variety of PV structures, such as rooftop and solar farm configurations, in a range of weather situations, including bright, overcast, and rainy ones, during the summer, fall, spring, and winter seasons. According to the recording device characteristics, the thermal images are available in a variety of formats (usually 640×480, 800×600, and 1024×768). Supervised training for fault identification is made possible by labeling the images into several fault

TABLE 1. Dataset Description

Dataset attribute	Description
Dataset Name	PV Thermal Imaging Fault Dataset
Data Source	UAV-based thermal images from PV panels, collected under diverse environmental conditions
Data Type	Thermal images (Infrared)
Resolution	Varies between 640×480, 800×600, and 1024×768 depending on the UAV camera used
Number of Images	10,000+ images
Fault Types	Hot spots, microcracks, electrical faults, and panel malfunctions
Image Format	JPEG, PNG, TIFF
Timeframe	Across all four seasons (spring, summer, fall, winter)
Environmental Conditions	Various lighting, temperature, and weather conditions (cloudy, sunny, rainy, etc.)
Annotation Type	Labelled for faults (e.g., hot spots, cracked cells, or no fault)
Data Collection Frequency	Regular intervals (e.g., every 5 minutes or hourly) depending on the setup
Data Augmentation	Includes flipping, rotating, and scaling to improve model robustness
Data Preprocessing	Normalization, noise reduction, and image resizing
Number of Classes	4 (Hot spot, Cracked cell, Electrical fault, No fault)
Data Collection Tool	UAV with infrared thermographic camera (e.g., FLIR, DJI)
Geographical Region	Various locations with diverse solar panel installations (e.g., rooftops, solar farms)
Temporal Data	Image sequences showing thermal dynamics over time (temporal sequence for fault progression analysis)
Labeling Method	Expert annotation based on thermal images and visual inspection

TABLE 2. Sample Data

Image ID	Fault Type	Resolution	Time of Capture	Environment	Temperature (°C)	Location	Annotations
001	Hot Spot	640×480	2024- 07-02 10:45 AM	Sunny	36ºC	Rooftop, City A	Hot spot in the middle of the panel
002	Cracked Cell	800×600	2024- 07-02 10:50 AM	Cloudy	29ºC	Rooftop, City B	Crack visible in top left corner
003	Electrical Fault	1024×768	2024- 07-02 10:55 AM	Sunny	36ºC	Solar Farm, City C	Electrical fault near junction box
004	No Fault	640×480	2024- 07-02 11:00 AM	Rainy	29ºC	Rooftop, City D	No anomalies detected
005	Hot Spot	800×600	2024- 07-02 11:05 AM	Sunny	37ºC	Solar Farm, City A	Hot spot near bottom right corner
006	Cracked Cell	640×480	2024- 07-02 11:10 AM	Cloudy	30ºC	Rooftop, City B	Crack visible in bottom right
007	Electrical Fault	1024×768	2024- 07-02 11:15 AM	Sunny	37ºC	Solar Farm, City C	Electrical fault along wiring

groupings, including electrical problems, hot spots, microcracks, and non-faulty panels (no fault).

The collection allows for longitudinal investigation of fault propagation since it contains both static thermal images and image sequences taken over time. Experts interpret the information according to discernible thermal anomalies in the images, and information enrichment methods like flipping, revolving, and scaling are used to improve the resilience of the mathematical framework. To get the images ready for deep learning, designs methods of preprocessing such as noise elimination and standardization are used. This dataset's mixture of time and space-based information enables the creation of deep learning examples. Notably, DRCNN efficiently detects and forecasts PV system errors, enhancing preservation and prolonging the panels' operational life. Sample data are shown in Table 2.

Deep learning models for PV panel defect diagnosis may be trained using this sample information, which offers an organized and transparent view of the characteristics linked to each thermal image in the dataset. An example of the gathered images is displayed in Fig. 4(a) and (b). The shading effect, shunted, dust-accumulated, and broken bypass diode are all normal problems seen in PV modules.

B. Image Pre-processing

Image preprocessing is an essential step in the analysis of PV panel defects using DRCNN. Enhancing image

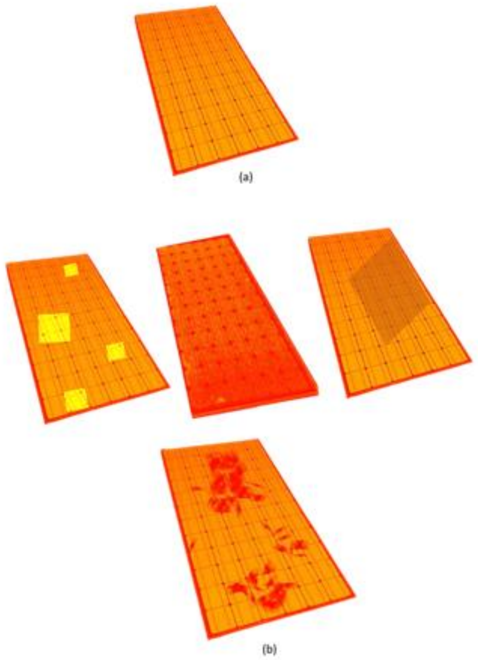

Fig. 4. Sample images of IRT: healthy(a) and faulty(b)

quality, lowering noise, normalizing the values of pixels, and preparing the information for neural networks to receive input are the objectives of image preprocessing.

1) Resizing

It is essential that all images have a uniform size for batch processing in deep learning models. Thermal images from UAVs may have different dimensions, and resizing is done to maintain consistency:

$$X_{resized} = f\left(X,(W,H)\right), \quad (1)$$

where X is the original image; W, H are the desired width and height, respectively; $f(X, (W, H))$ represents the resizing function.

2) Normalization

Normalization of pixel values is a technique to scale the values to a specific range, often between 0 and 1, which helps speed up the convergence of the model during training:

$$X_{norm}\left(i,j\right)=\frac{X\left(i,j\right)-X_{\min}}{X_{\max}-X_{\min}}, \quad (2)$$

where $X\left(i,j\right)$ is the pixel value at position $\left(i,j\right)$ in the image; $X_{\min}$ and $X_{\max}$ are the minimum and maximum pixel values in the image, respectively; $X_{norm}\left(i,j\right)$ is the normalized pixel value.

TABLE 3. Specifications of the Solar Power Grid

Power production rate in 2022	500 kW
Installation type	Ground mount
Panels type	Polycrystalline
Inverter type	String inverters
Commissioned	2019
CO_2 abated per year	747 tonnes
Equivalent to planting	12 910 Trees

3) Grayscale Conversion

Since thermal images are typically represented in grayscale, this step ensures that the image only contains intensity values, reducing computational complexity:

$$X_{grayscale}\left(i,j\right)=0.2989R\left(i,j\right)+ \\ +0.587G\left(i,j\right)+0.114B\left(i,j\right), \quad (3)$$

where $X_{grayscale}\left(i,j\right)$ is the resulting grayscale intensity at pixel $\left(i,j\right)$.For thermal images, the RGB channels might already be collapsed into a single channel, so this step might be skipped.

4) Noise Reduction

Thermal images often contain noise due to environmental factors. A common method to reduce noise is applying Gaussian filtering, which smooths the image and removes high-frequency noise:

$$X_{filtered}\left(i,j\right)=\sum_{x=-k}^{k}\sum_{y=-k}^{k}G\left(x,y\right)X\left(i+x,j+y\right), \quad (4)$$

where $G\left(x,y\right)$ is the Gaussian kernel; $X\left(i+x,j+y\right)$ is the pixel value at the neighborhood of pixel $\left(x,y\right)$; k defines the size of the kernel (e.g., 3×3 or 5×5).

5) Data Augmentation

Rotation:

$$X_{rotated}\left(i',j'\right)=X\left(R^{-1}\left(i',j'\right)\right), \quad (5)$$

where R^{-1} is the inverse rotation matrix used to rotate the image by a certain angle.

Flipping:

$$X_{flipped}\left(i,j\right)=X\left(W-i,j\right), \quad (6)$$

where W is the width of the image.

Scaling:

$$X_{scaled}\left(i,j\right)=X\left(\alpha i,\alpha j\right), \quad (7)$$

where α is the scaling factor.

6) Edge Detection

It can be used to highlight important features such as cracks or hot spots. One of the most common techniques is

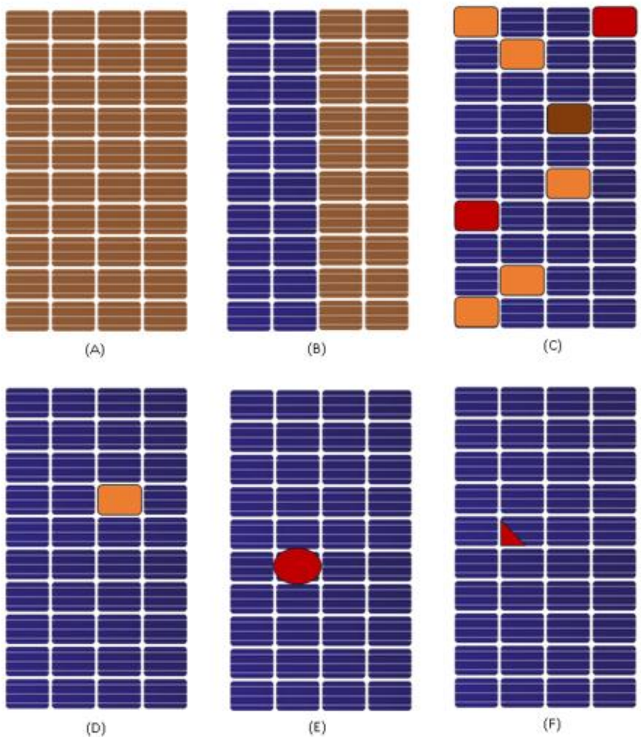

Fig.5.Different PV faults in thermography: Open circuit (offline)(a); Bypass diode short circuit panel (b); Shading represents wrong connection (c); Defect cell or shading (delamination) (d); Snail trails (Pointed heat) (e); Broken cell (f).

the Sobel operator:

$$X_{edge}(i,j)=\sqrt{\left(\frac{\partial X}{\partial x}\right)^2+\left(\frac{\partial X}{\partial j}\right)^2}, \tag{8}$$

where $\frac{\partial X}{\partial x}$ and $\frac{\partial X}{\partial j}$ are the gradients of the image in the x and y directions.

7) Final Preprocessed Image

After the preprocessing steps, the final preprocessed image is ready for input into the DRCNN model:

$$X_{final}(i,j)= = f_{final}\left(X_{resized}, X_{norm}, X_{grayscale}, X_{filtered}, X_{edge}\right), \tag{9}$$

where X_{final} denotes the composite function that applies all preprocessing steps in a sequence.

These preprocessing techniques help enhance the quality and consistency of the thermal images, which is crucial to identify faults in PV panels using the proposed DRCNN system.

C. Specifications

1) Solar Power Grid

The specifications of a 500 kW solar power grid, which occupies an area of around 1 200 m2, is shown in Table 3.

2) Thermal Camera Specifications

Large power plants frequently utilize IRT for non-contact temperature analysis and measurement. IR cameras offer several advantages over manual inspections, including the ability to record temperature data remotely and display temperature patterns instantly. When employing IRT for PV power plant analysis, certain requirements, limitations, and factors must be considered. The ability of an infrared camera to detect minute temperature variations is referred to as its sensitivity; higher sensitivity enables the detection of smaller temperature changes. In addition, the precision of a thermal imaging camera reflects its ability to provide consistent and accurate temperature readings under repeated measurements. The number of pixels in the camera's sensor, or resolution, also influences the quality of thermal images. Cameras with higher sensitivity, precision, and resolution provide more reliable and accurate temperature assessments.

D. Visual Thermal Methods (VTMs)

Figure 5(a)–(f) illustrates six distinct thermal signatures commonly observed in PV modules through thermographic inspection. These thermal images provide a visual representation of surface temperature variations, where color gradients indicate differences in heat distribution. Warmer zones typically appearing in red, orange, or brown, highlight the presence of faults or defects. Figure 5(a) displays a module that is uniformly warm, indicating an open circuit or offline status. Figure 5(b) presents a characteristic pattern caused by a short-circuited bypass diode that affects a defined section of cells. Figure 5(c) shows irregular warming attributed to shading effects or improper electrical connections. Figure 5(d) highlights an isolated hot spot, often linked to a single defective cell or delamination. Figure 5(e) captures localized heating associated with snail trails or concentrated pointed defects. Figure 5(f) depicts the triangular thermal pattern of a broken cell. These panels provide a practical reference for identifying and classifying PV module failures based on distinctive thermal signatures, thereby supporting fault detection and predictive maintenance strategies in solar energy systems.

E. Feature Extraction Using DRCNN

To prevent the explicit collection of characteristics, the DRCNN–a multilayer neural network –has demonstrated outstanding results in hyperspectral image recognition, as illustrated in the training data shown in Fig. 6. To improve the outcomes, the cross-entropy derived from gradient research and the loss function are analyzed simultaneously. MNIST and CIFAR-10 are two deep-learning benchmark datasets that were used in the studies. In both datasets, the proposed DRCNN produced useful outcomes. When it comes to illustrating and classifying the characteristics of images, they are unmatched.

Imperfection diagnosis and defect detection are the two primary tasks of the process shown in Fig. 7. Classifying

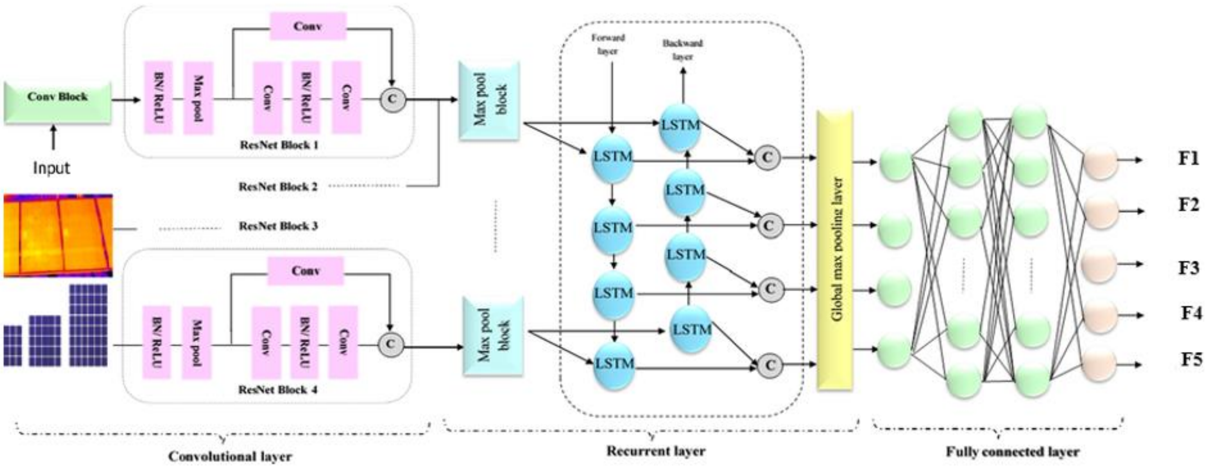

Fig. 6. DRCNN-based classification for fault identification in PV Panels using thermal imaging.

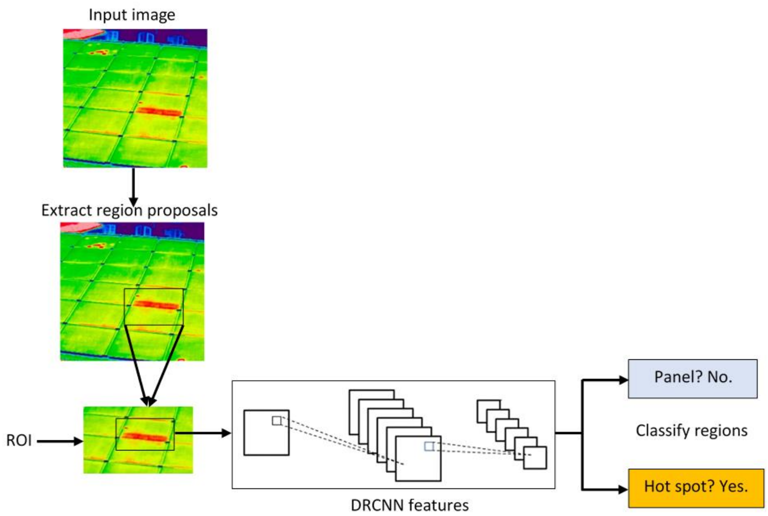

Fig.7.Fault identification using DRCNN. The DRCNN algorithm for identification of faults in photovoltaic panels through the use of thermal imaging.

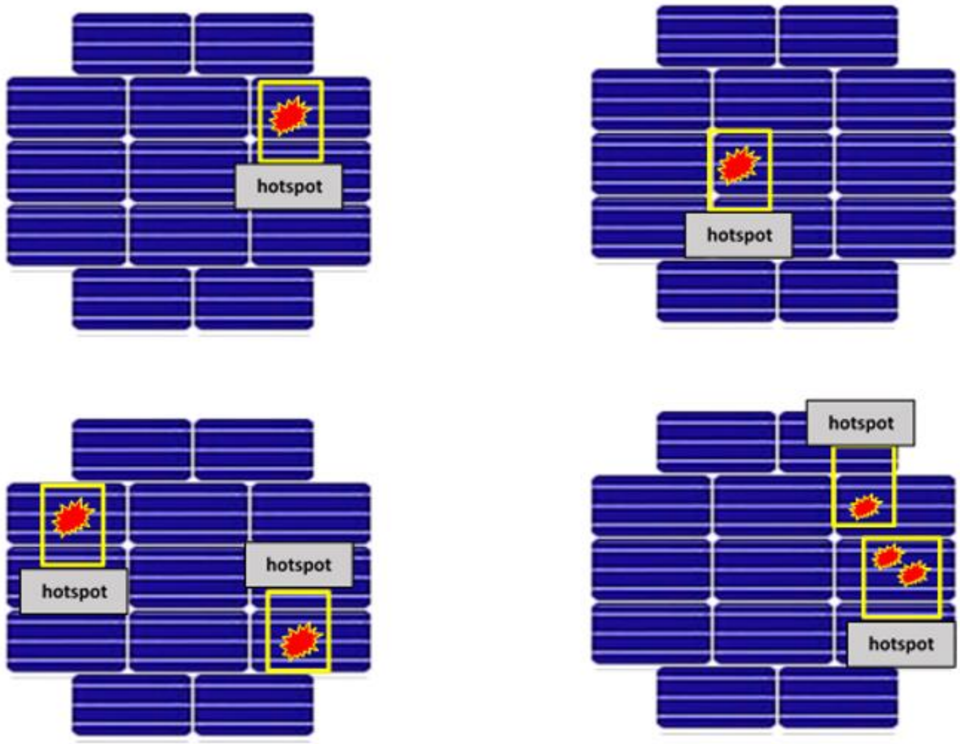

Fig. 8.Region of interest for DRCNN training.

the studied defects is the purpose of the fault diagnostic function, whereas fault detection seeks to identify abnormalities in the PV cells. Every defect has a unique temperature and this process is based on looking at the differences in the hotspot profile.

Step 1: Prepare input data

Thermal Image Acquisition. Collect thermal images of photovoltaic panels using UAVs under various environmental conditions.

Preprocessing. Enhance the images through resizing, normalization, noise reduction, and augmentation:

$$X_{preprocessed} = f\left(X\right), \tag{10}$$

where X is the original image, and f represents the sequence of preprocessing operations.

Step 2: Extract features using convolutional layers

Convolution Operation. Extract spatial features from the thermal images using convolutional filters:

$$F\left(i, j,k\right) = \sum_{x=1}^{m}\sum_{y=1}^{n} X\left(i+x, j+y\right) W(x,y,k) + b\left(k\right), \tag{11}$$

where $F\left(i, j, k\right)$ is the feature map at position (i, j) for filter k; $W\left(x, y,k\right)$ is the weight of the filter; $b(k)$ is the bias term; m and n are the dimensions of the filter.

Activation Function. Apply a non-linear activation function, such as ReLU, to introduce non- linearity:

$$F_{activated}\left(i, j,k\right) = \max\left(0, F\left(i, j,k\right)\right). \tag{12}$$

Pooling Operation. Downsample the feature maps to reduce dimensionality and computational load:

$$\begin{gathered} P\left(i, j,k\right) = \max\left(F_{activated}\left(i', j',k\right)\right), \\ \forall\left(i', j'\right) \in pooling\ window, \end{gathered} \tag{13}$$

where $P\left(i, j, k\right)$ is the pooled output value at position (i, j) for the feature map channel k. The $F_{activated}\left(i', j', k\right)$ represents the ReLU-activated feature values inside the pooling window corresponding to location (i, j). The operator max selects the maximum value within the pooling window.

Step 3: Extract temporal features using recurrent layers

Sequence Formation. Flatten spatial features into a sequence of feature vectors:

$$S_t = Flatten\left(P_t\right), \tag{14}$$

where S_t is the feature vector at time t, and P_t is the pooled feature map at time t.

Recurrent Neural Network (RNN) operation. Use Long Short-Term Memory (LSTM) units or Gated Recurrent Units (GRU) to capture temporal dependencies. LSTM cell

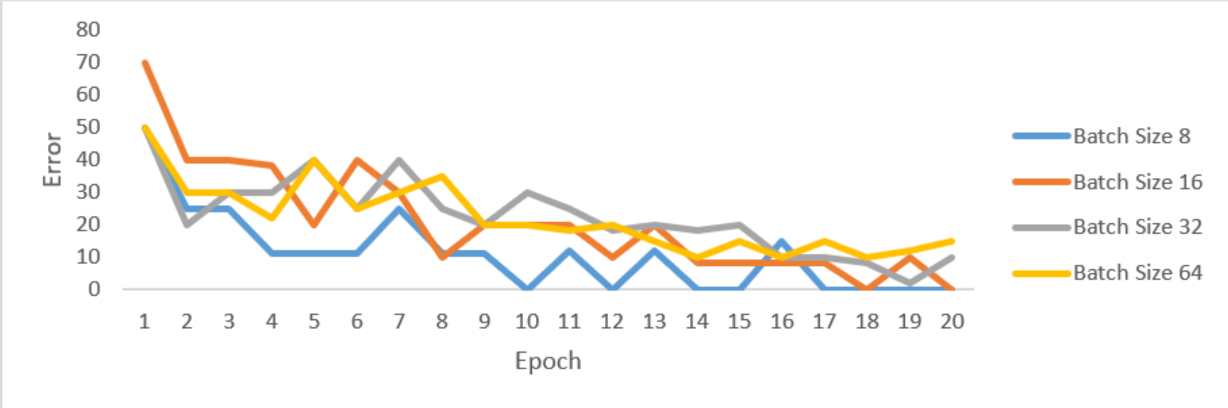

Fig. 9. Comparison of error vs maximum epoch during DRCNN validation.

equations:

$$f_t = \sigma\left(W_f\left[h_{t-1}, S_t\right] + b_f\right), \tag{15}$$

$$\tilde{C}_t = \tanh\left(W_C\left[h_{t-1}, S_t\right] + b_C\right), \tag{16}$$

$$C_t = f_t C_{t-1} + x_t \tilde{C}_t, \tag{17}$$

$$o_t = \sigma\left(W_o\left[h_{t-1}, S_t\right] + b_o\right), \tag{18}$$

$$h_t = o_t \tanh\left(C_t\right), \tag{19}$$

where f_t, x_t, o_t stand for the forget, input, and output gates, respectively; C_t is the cell state; h_t represents the hidden state; S_t is the input vector, W_f, b_f are the weight max and the bias term of the forget gate, respectively; σ is the sigmoid activation function, W_C, b_C are the weight matrix and the bias for a candidate cell state, respectively; $\tanh$ is the hyperbolic tangent activation function; W_o, b_o are the output gate values of the weight matrix and the bias, respectively; t–1 indicates the pervious state in relation to the current state; $\tilde{C}_t$ is the candidate new cell state.

Step 4: Classify

Fully connected layer. Map the extracted features to fault classes:

$$z = W_{fc} h_T + b_{fc}, \tag{20}$$

where h_T is the hidden state at the last time step; W_{fc} represents the weights of the fully connected layer; b_{fc} is the bias term.

Softmax Function. Compute the probabilities of fault categories:

$$p\left(c\right) = \frac{e^{z_c}}{\sum_y e^{z_y}}, \tag{21}$$

where $p(c)$ is the probability of class c; z_c is the output score for class c.

Step 5: Calculate loss function

Categorical Cross-Entropy Loss:

$$L = -\frac{1}{N}\sum_{x=1}^{N}\sum_{c=1}^{C} y_{x,c} \log\left(p_{x,c}\right), \tag{22}$$

where N is the number of samples; C is the number of classes; $y_{x,c}$ is the true label of sample i for class c; $p_{x,c}$ is the predicted probability of sample i for class c.

The proposed DRCNN algorithm is designed for automated fault identification in photovoltaic panels using thermal imaging. In the first stage, UAV-acquired thermal images are preprocessed through resizing, normalization, noise reduction, and augmentation to enhance data quality. Spatial features are then extracted using convolutional layers, where convolution, activation (ReLU), and pooling operations capture localized fault-related patterns while reducing dimensionality. These spatial features are flattened into sequential vectors and processed through recurrent layers, such as LSTM or GRU units, to model temporal dependencies and identify subtle variations in thermal signatures. The final hidden state is passed through a fully connected layer, and the Softmax function assigns probabilities to fault categories, enabling accurate classification of different defect types. Model learning is guided by categorical cross-entropy loss, ensuring optimized prediction accuracy across multiple fault classes. This integration of CNN-based spatial analysis with RNN-based temporal modeling ensures robust and precise detection of PV faults under diverse environmental conditions.

TABLE 4. Performance Measures

System	Accuracy (%)	Precision (%)	Recall (%)	F1-Score (%)
DRCNN	99.8	99.6	99.0	99.8
CNN-based approach	95.6	94.3	93.9	94.0
LSTM-based method	94.8	93.6	95.0	94.3
SVM with feature selection	92.5	91.9	90.1	91.4
RNN	96.9	96.0	96.4	96.2

TABLE 5. Performance Measures (Error)

System	MAE	MSE	RMSE
DRCNN	0.013	0.0016	0.040
CNN-Based Approach	0.026	0.0033	0.058
LSTM-Based Method	0.023	0.0029	0.054
SVM with Feature Selection	0.031	0.0046	0.068
RNN Model	0.019	0.0021	0.046

IV. RESULTS AND DISCUSSIONS

The GUI-powered system in the proposed studies for hotspot detection on electrical lines and fuses will look at two different kinds of faults: 1) excess temperatures in the fuse contact and 2) excessive temperatures in any one or two electrical segments.

320 hotspots are included in the 800 images that make up the training image set that is used. It is necessary to incorporate various panel kinds, forms, sizes, and alignments. In this study, the instruction procedure was carried out by identifying the Region of Interest (ROIs) within the selected frames of each subject. Two kinds of ROIs are examined: ROIs for a panel set and relative hot spots. The border-box and labeling must be defined before the ROIs may be created. The region of the image covered by the ROI is identified by the border-box. An illustration of the ROIs during the DRCNN training procedure is provided in Fig. 8.

Figure 9 illustrates the validation error across 20 epochs for the DRCNN algorithm, comparing the performance of four different batch sizes: 8, 16, 32, and 64. The general trend is that error decreases as the number of epochs increases, though all models exhibit significant volatility, particularly the Batch Size 8 model. The Batch Size 16 model demonstrates the lowest final error, while the Batch Size 32 model shows the least volatility after the initial epochs. The results are comparable based on the observation that the inaccuracy stabilizes for most models after approximately 15 epochs.

Figure 10(a) shows the original image. Figure 10(b) demonstrates the result of whatever process is described for 10(b) (e.g., edge detection, filtering, etc.). The current B&W image seems to be an edge detection output. Figure 10(c)definitively shows the rotated version of the image from 10(a) or the processed version from Fig. 10(b), depending on the workflow. Figures 10(d), 10(e), and 10(f) are unique representations of their specific processing step (panel detection, hot area detection, and final prediction), even if the differences are subtle (e.g., different bounding boxes, masks, or overlay colors). The image duplication invalidates the entire sequence.

The proposed DRCNN system achieves the highest performance across all metrics due to its integrated spatial and temporal feature extraction capabilities shown in Table 4. The RNN model performs well but slightly lags behind the proposed system, as it may not fully capture complex dependencies. Existing models, such as SVM, show the lowest performance indicating limitations in handling the large feature space and temporal dependencies. The proposed DRCNN system achieves the lowest errors (MAE, MSE, and RMSE), demonstrating superior prediction accuracy. The RNN model performs well but is slightly less effective than the proposed system. The SVM with feature selection has the highest errors, showing its limitations in capturing complex patterns in data.

The changes in the learning impairment and precision functions are displayed in Fig. 11(a). The degree of precision is very close to 1 and the loss is as low as 0.01. The matrix of confusion that was generated is shown in Fig. 11(b).

V. CONCLUSION

When employing IRT to detect faults in PV solar panels, the DRCNN demonstrates significant improvements in precision, recall, F1-score, and accuracy compared to existing techniques. The proposed model effectively captures the complex thermal characteristics of defective panels under various conditions by leveraging RCNN for temporal pattern recognition and CNN for spatial feature extraction. Superior performance metrics, such as reduced

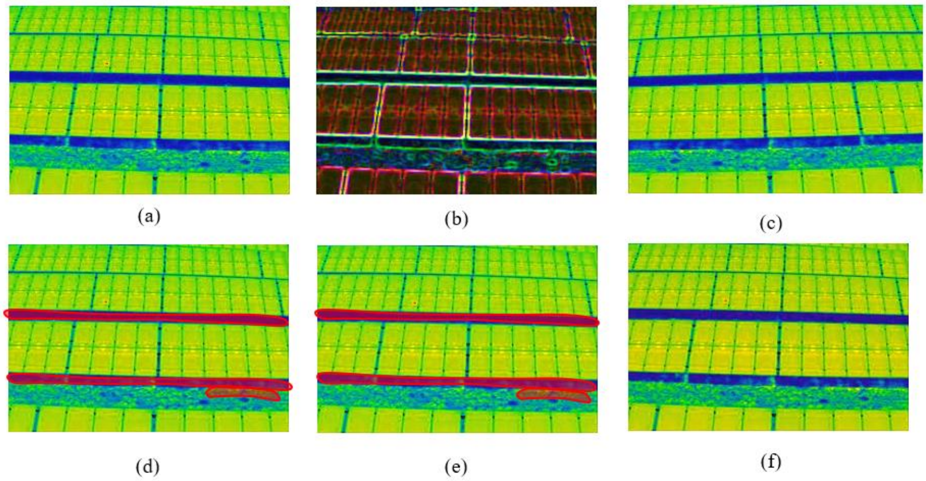

Fig. 10. IRT (a), Detection of contour (b); Image rotation (c), Panel detection (d); Detection of hot region (relative) (e); Location of relative hotter regions (f).

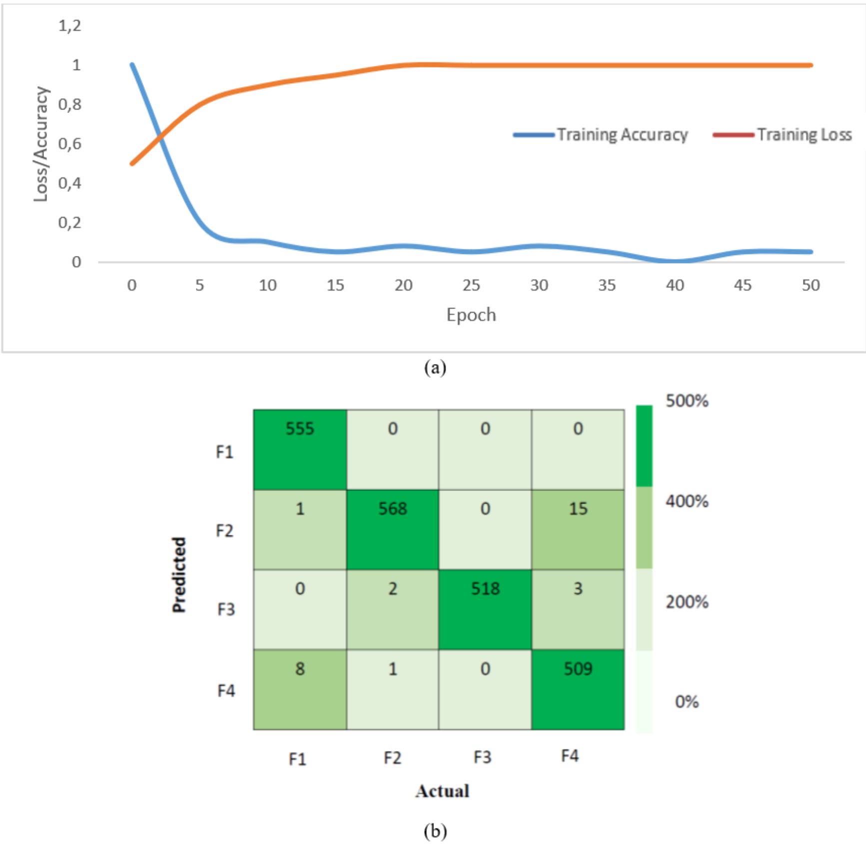

Fig. 11. Multiclass classification (fault diagnosis): training loss and accuracy functions (a); confusion matrix (b).

Mean Absolute Error (MAE), Mean Squared Error (MSE), and Root Mean Squared Error (RMSE), indicate that the integration of advanced preprocessing techniques with a robust architectural design minimizes error rates. This approach enhances defect detection, contributing to improved energy utilization and reduced operational costs. It offers a scalable solution for real-time solar system monitoring and maintenance. The results provide a solid foundation for future research in automated fault diagnostic systems and underscore the potential of deep learning frameworks in advancing green energy technology.

References

[1] Ö.Baltacı, Z.Kıral, K.Dalkılınç, O.Karaman, "Thermal image and inverter data analysis for fault detection and diagnosis of PV systems,"Applied Sciences, vol. 14, no. 9, Art. no. 3671, 2024.

[2] S. Umar, M. S. Qureshi, M. U. Nawaz, "Thermal Imaging and AI in solar panel defect Identification," International Journal of Advanced Engineering Technologies and Innovations, vol. 1, no. 3, pp. 73–95, 2024.

[3] Z. Tang, X. Jian, "Thermal fault diagnosis of complex electrical equipment based on infrared image recognition," Scientific Reports, vol. 14, no. 1, Art. no. 5547, 2024.

[4] G. B.Balachandran, M.Devisridhivyadharshini, M. E.Ramachandran, R. Santhiya, "Comparative investigation of imaging techniques, pre-processing and visual fault diagnosis using artificial intelligence models for solar photovoltaic system–A comprehensive review," Measurement, vol. 232, Art. no. 114683, 2024.

[5] W. Zhang, G. Wang, G. Yao, C. Lu, Y. Liu, "Study on fault monitoring technology of photovoltaic panel based on thermal infrared and optical remote sensing," The International Archives of the Photogrammetry, Remote Sensing and Spatial Information Sciences, vol. 48, pp. 855–860, 2024.

[6] C. Yang, F. Sun, Y. Zou, Z. Lv, L. Xue, C. Jiang, H. Cui, "A survey of photovoltaic panel overlay and fault detection methods," Energies,vol. 17, no. 4, Art. no. 837, 2024.

[7] H. Yousif, Z. Al-Milaji, "Fault detection from PV images using hybrid deep learning model," Solar Energy, vol. 267, Art. no. 112207, 2024.

[8] Prakasam, K. R. Laxmikanth, P. Srinivasu, "Design and simulation of circular microstrip patch antenna with line feed wireless communication application," in 2020 4th International Conference on Intelligent Computing and Control Systems (ICICCS), Madurai, India, 2020, pp. 279–284.DOI: 10.1109/ICICCS48265.2020.9121162.

[9] S. Jaybhaye, V. Sirvi, S. Srivastava, V. Loya, V. Gujarathi, V. D. Jaybhaye, "Classification and early detection of solar panel faults with deep neural network using aerial and electroluminescence images," Journal of Failure Analysis and Prevention, vol. 24, pp. 1746–1758, 2024.

[10] X. Chao, L. Zhang, Y. Li, C. Huang, J. Li, "Photovoltaic fault detection based on infrared and visible image augmentation and fusion," Turkish Journal of Agriculture and Forestry, vol. 48, no. (3), pp. 430–442, 2024.

[11] U. Shafique, S. M. Alam, U. Rashid, W. Javed, H. Anwaar, M. S. Zeb, F. Nzanywayingoma, "Infrared thermography based insulator fault classification via unsupervised clustering and semi-supervised learning," IEEE Access, vol. 12, pp. 180781–180791,2024.

[12] X. Zhang, Y. Ge, Y. Wang, J. Wang, W. Wang, L. Lu, "Residual learning-based robotic image analysis model for low-voltage distributed photovoltaic fault identification and positioning," Frontiers in Neurorobotics, vol. 18, Art. no. 1396979, 2024.

[13] P. Garikapati, K. Balamurugan, T. P. Latchoumi, R. Malkapuram, "A cluster-profile comparative study on machining AlSi7/63% of SiC hybrid composite using agglomerative hierarchical clustering and K-means," Silicon, vol. 13, no. 4, pp. 961–972, 2021.

[14] P. Chandana, P. G. S. Ghantasala, J. Rethna Virgil Jeny, K. Sekaran, N. Deepika, Y. Nam, S. Kadry, "An effective identification of crop diseases using faster region-based convolutional neural network and expert systems,"International Journal of Electrical and Computer Engineering, vol.10, no. 6, pp. 6531–6540, 2020. DOI: 10.11591/IJECE.V10I6.PP6531-6540.

[15] M.Rama Krishna, K. R.Tej Kumar, G. Durga Sukumar, "Antireflection nanocomposite coating on PV panel to improve power at maximum power point,"Energy Sources, Part A: Recovery, Utilization and Environmental Effects, vol. 40, no. 21, pp. 2407–2414, 2018. DOI: 10.1080/15567036.2018.1496198.

[16] G. Tanda, M. Migliazzi, "Infrared thermography monitoring of solar photovoltaic systems: A comparison between UAV and aircraft remote sensing platforms," Thermal Science and Engineering Progress,vol. 48, Art. no. 102379, 2024.

[17] E. A.Ramadan, N. M.Moawad, B. A.Abouzalm, A. A.Sakr, W. F.Abouzaid, G. M. El-Banby, "An innovative transformer neural network for fault detection and classification for photovoltaic modules," Energy Conversion and Management,vol. 314, Art. no. 118718, 2024.

[18] C.Kim, S. Perilli, S. Sfarra, E. J. Kim, "Detection of the surface coating of photovoltaic panels using drone-acquired thermal image sequences," Journal of Thermal Analysis and Calorimetry,vol. 149, no. 8, pp. 3443–3452, 2024.

[19] E. K.Ukiwe, S. A. Adeshina, T.Jacob, B. B. Adetokun, "Deep learning model for detection of hotspots using infrared thermographic images of electrical installations," Journal of Electrical Systems and Information Technology,vol. 11, no. (1),Art. no. 24, 2024.

[20] R. Duan, Z. Ma, "A method for detecting photovoltaic panel faults using a drone equipped with a multispectral camera," ISPRS Annals of the Photogrammetry, Remote Sensing and Spatial Information Sciences, vol. 10, pp. 59–65, 2024.

[21] K. Awedat, G. Comert, M. Ayad, A. Mrebit, "Advanced fault detection in photovoltaic panels using enhanced U-Net architectures," Machine Learning with Applications, vol. 20, Art. no. 100636, 2025.

[22] U. R.Qureshi, A.Rashid, N.Altini, V.Bevilacqua, M. La Scala, "Radiometric infrared thermography of solar photovoltaic systems: An explainable predictive maintenance approach for remote aerial diagnostic monitoring," Smart Cities,vol. 7, no. 3, pp. 1261–1288, 2024.

[23] N. V.Sridharan, V.Sugumaran, "Visual fault detection in photovoltaic modules using decision tree algorithms with deep learning features," Energy Sources, Part A: Recovery, Utilization, and Environmental Effects,vol. 47, no. 2, Art. no. 2020379, 2025.

[24] D. Matusz-Kalász, I. Bodnár, M. Jobbágy, "An overview of CNN-based image analysis in solar cells, photovoltaic modules, and power plants," Applied Sciences,vol. 15, no. 10, Art. no. 5511, 2025.

[25] Cardoso, D. Jurado-Rodríguez, A. López, M. I. Ramos, J. M. Jurado, "Automated detection and tracking of photovoltaic modules from 3D remote sensing data," Applied Energy,vol. 367,Art. no. 123242, 2024.

[26] P. Sandeep, P. A. Harsha Vardhini, V. Prakasam, "SRAM utilization and power consumption analysis for low power applications," in 2020 International Conference on Recent Trends on Electronics, Information, Communication & Technology (RTEICT), Bangalore, India, 2020, pp. 227–231. DOI: 10.1109/RTEICT49044.2020.9315558.

[27] D. Suárez-Gómez, J. O. B. Quintero, "Integrated thermal monitoring system for solar PV panels: An approach based on TinyML and Edge Computing," in Workshops at the 7th International Conference on Applied Informatics 2024 (ICAIW 2024), Oct. 24–26, 2024, Viña del Mar, Chile, pp. 14–27.

[28] W. Yang, W. Wang, X. Wang, J. Gu, Z. Wang, "Fault diagnosis method of a cascaded H-bridge inverter based on a multisource adaptive fusion CNN-transformer," IET Power Electronics,2024, pp. 1–21.

[29] S. K.NB, S. Madichetty, S. S. Koduru, M. V. S. P. Chowdary, S. Mishra, "Finding a faulty/partially shaded panel in an solar photovoltaic array: A novel and instantaneous additional hardware module-based echnique," IEEE Industry Applications Magazine, vol. 31, no. 1, pp. 73–85, 2025.